Available online at www.sciencedirect.com

ScienceDirect

Polymer 48 (2007) 6681–6690

polymer

www.elsevier.com/locate/polymer

Dynamic viscoelastic behavior of triple helical Lentinan in water: Effects of concentration and molecular weight

Yangyang Zhang, Xiaojuan Xu*, Juan Xu, Lina Zhang

Department of Chemistry, Wuhan University, Wuhan 430072, China

Received 22 May 2007; received in revised form 1 August 2007; accepted 1 September 2007
Available online 6 September 2007

Abstract

The dynamic viscoelasitc behavior of Lentinan, one triple helical β-(1 → 3)-D-glucan from the fruiting body of *Lentinus edodes*, in water was investigated as a function of concentration and molecular weight at 25 °C by using dynamic rheology. It was revealed that the shear storage moduli (G'), viscous loss moduli (G''), and the dynamic complex viscosity (η^*) exhibited strong dependence on concentration and molecular weight. At low concentrations, the Lentinan/water systems displayed liquid-like behavior with G' lower than G'' at low frequencies and crossing-over at high frequencies. With increasing concentration, the elastic response of the Lentinan/water system was stronger than the viscous response, leading to the conclusion that the Lentinan/water systems displayed a predominantly solid-like behavior. The gel point (c_{gel}) was determined from Winter–Chambon method (frequency-independence of tan δ). The most important point is that the c_{gel} was much lower than some synthesized polymers and other flexible polysaccharides, which may be attributable to the high stiffness of triple helical Lentinan and strong intra- and intermolecular interactions among polysaccharide chains. Furthermore, a decrease in molecular weight leads to a sharp increase of c_{gel}. The dynamic strain sweep measurements proved that the gelation of Lentinan in water is induced by the extremely entangled and stiff triple helices forming continuous network, and the Lentinan gel is structurally more like a solution that is unable to flow within a timescale of usual observation.

Keywords: Triple helical Lentinan; Dynamic viscoelastic behavior; Solution–gel transition

1. Introduction

In the past two decades, the naturally occurring polysaccharides have received much attention because of their wide applicability in industries as texture modifiers, gelling agents, thickeners, emulsifiers, stabilizers and coating or packaging films in various fields including foods, pharmaceuticals, cosmetics, textiles and biomedical sectors [1,2]. Gellan and xanthan gums are the most commonly applied for commercial importance, and have been produced in a large scale by industrial fermentation. Gellan gum has been expected to be not only a new gelling agent but also a good model for the study of thermo-reversible gelling process. However, it is not a gel-forming polysaccharide, but forms a transparent gel resistant to acid and heat in the presence of divalent cations [3]. Xanthan is also a non-gelling polysaccharide that can exist in solution as a rigid and ordered chain conformation, and show shear-thinning flow behavior in concentrated solution. When it is mixed with other non-gelling polysaccharides of the galactomannan family, it can form gels. Therefore, it is used as thickening agent now, and the rheological properties of the gels formed from xanthan mixed with other non-gelling polysaccharides of the galactomannan family have been the object of extensive research [4–7].

Polysaccharides from fungi are an interesting source of additives for several industries, in particular for the food and pharmaceutical industries because of their safe and nonpoisonous functional properties in a variety of products. Lentinan,

---

* Corresponding author. Tel.: +86 27 87219274; fax: +86 27 68754067.
E-mail address: xuxj626@263.net (X. Xu).

0032-3861/$ - see front matter © 2007 Elsevier Ltd. All rights reserved.
doi:10.1016/j.polymer.2007.09.005

which is a neutral polysaccharide produced by *Lentinus edodes*, consists of a β-(1 → 3)-D-glucan with a side chain of β-(1 → 6)-D-glucan [8]. Lentinan occurs as triple helix in aqueous solution [9], and it transits from triple helix to random coils in aqueous solutions containing dimethyl sulfoxide (DMSO) or concentrated NaOH solution [10,11]. Interestingly, it is different from the non-gelling polysaccharides such as gellan and xanthan gums that Lentinan in water can form a gel at room temperature without addition of anything. However, to our knowledge, a rheological characterization of Lentinan in aqueous systems has been scarcely published. The study of gelation of polysaccharides is not only scientifically interesting but also important in food, pharmaceutical, biomedical, cosmetic, coating, painting, and related industries [12]. Therefore, the aim of this paper is to present a thorough investigation of the dynamic viscoelastic properties of Lentinan aqueous systems under different polymer concentration conditions to clarify the solution–gel transition process in water. This work will provide important information of rheology for stiff polysaccharides, and contribute to application of natural polysaccharides in industry.

Dynamic rheology is one of the most extensive methods to study rheological properties of polysaccharide solution. The rheological characteristics in the vicinity of the solution–gel transition can be described using the power laws or scaling laws [13–15]. Three scaling laws, which have been extensively applied to many types of polymeric gels (both chemical and physical gels), are established for (i) the zero-shear viscosity η_0 [16–18], (ii) the dynamic moduli G' and G'' [19–23], and (iii) the equilibrium modulus G_e before, at, and beyond the solution–gel transition, respectively [24–26].

$$\eta_0 \propto \varepsilon^{-\gamma} \qquad \text{for } p < p_g \tag{1}$$

$$G'(\omega) \cong G''(\omega) \propto \omega^n \qquad \text{at } p_g \tag{2}$$

$$G_e \propto \varepsilon^z \qquad \text{for } p > p_g \tag{3}$$

where $\varepsilon = |p - p_g|/p_g$ is the relative distance of a gelling variable p departing from the solution–gel transition point p_g, and p can be, for example, the degree of cross-linking, gelation time, gelation concentration, or gelation temperature in a gelation process; ω is the angular frequency; γ, n and z are the critical exponents determining the critical characteristics in the vicinity of the solution–gel transition, which have been predicted theoretically by many models [26]. The three indexes for the scaling laws are always positive. The critical exponent n theoretically ranges from 0 to 1. The typical experimental values of γ are between about 1.3 and 1.7, and the typically reported values of z are to be 2.0–3.0 [26]. This approach defines a critical gel point, p_g, where G' and G'' exhibit the same power law dependence with frequency over a broad frequency range corresponding to the formation of a continuous network at the percolation threshold. This work will study the solution–gel transition of Lentinan and examine if the solution–gel transition behavior could be described by the scaling law proposed by Winter and Chambon.

2. Experimental section

2.1. Sample preparation

Lentinan was isolated from fruiting bodies of *L. edodes* cultivated in Fujian in China by extraction with 5% NaOH/0.05% $NaBH_4$ two times, and precipitation with 36% acetic acid to remove α-(1 → 3)-D-glucan, according to previously reported method [9]. The supernatant was treated with 30% H_2O_2 to decolorize. Aqueous solution of Lentinan was dialyzed against distilled water for 4 days, and concentrated by rotary evaporator at reduced pressure below 45 °C, and finally lyophilized to obtain colorless flakes coded as LF-1. In order to investigate the effect of molecular weight on the solution–gel transition, LF-1 was dissolved in water with concentration of 1.5 wt%, and degraded into three fractions by ultrasonic degradation performed on the Ultrasonic Cleaning Machine MUS/1004 (Shenzhen Modern Ultrasonic Industrial Co., Ltd., China) with different time such as 2, 4.5 and 10 h at 25 °C. The sample solutions were dialyzed, and lyophilized to get the final fractions coded as LF-2, LF-3, LF-4, respectively. The four samples LF-1–LF-4 were used in the following experiments.

2.2. Intrinsic viscosity

The intrinsic viscosities ($[\eta]$) of Lentinan fractions in water and dry dimethyl sulfoxide (DMSO) at 25 °C were determined by using an Ubbelohde capillary viscometer. All fractions have low critical overlap concentrations c^* at which the transition from a dilute solution of independently moving chains to a network occurred. For example, the c^* value for LF-1 has been estimated to be about 3.8×10^{-4} g/mL, and those for LF-2 and LF-3 are $\sim 1 \times 10^{-3}$ g/mL. Therefore, all the measurements were carried out in the dilute regimes ($c < c^*$). The kinetic energy was always negligible. The Huggins and Kraemer equations were used to estimate the intrinsic viscosity.

$$\frac{\eta_{sp}}{c} = [\eta] + k[\eta]^2 c \tag{4}$$

$$\frac{\ln \eta_r}{c} = [\eta] - \beta[\eta]^2 c \tag{5}$$

where η_{sp}/c is reduced viscosity; η_r, relative viscosity; c, polymer concentration with unit of g/mL; k and β, the constants for given polymer in desired conditions.

2.3. Light scattering

The light scattering intensities of Lentinan fractions in pure water (double distilled water) were determined by multi-angle laser light scattering instrument (MALLS) (Wyatt DAWN DSP, Santa Barbara, CA) at the angles of 26, 35, 43, 52, 60, 69, 80, 90, 100, 111, 121, 132, 142, 152, and 163° combined with size exclusion chromatogram (SEC-LLS) equipped with a TSK-gel G4000 PWXL column (7.8 mm × 300 mm), a TSK-gel G6000 PWXL column (7.8 mm × 300 mm), a differential refractometer (Wyatt Optilable DSP) at 25 °C with a polarized He–Ne laser of 633 nm in wavelength. The eluent was second distilled water with a flow rate of 0.8 mL/min. The solutions of desired polysaccharide concentrations were prepared, and optical clarification of the solutions was achieved by filtration through a sand filter followed by a 0.45 μm pore-size filter (NYL, 13 mm Syringe filter, Whatman, Inc., USA). The injection volume is 200 μL. The light scattering intensities of Lentinan in dry DMSO was measured by multi-angle laser light scattering instrument (MALLS) (Wyatt DAWN DSP, Santa Barbara, CA) at the angles of 49, 56, 63, 71, 81, 91, 99, 109, 118, and 127°. The angular and concentration-dependences of scattered intensities were analyzed by using Berry's square root plot [27], that is $(Kc/R_\theta)^{1/2}$ vs $\sin^2(\theta/2) + kc$. Here K is the optical constant, c the polymer mass concentration, k the "stretch factor," which scales the contributions from c to be roughly equal to the contributions from $\sin^2(\theta/2)$, and R_θ the reduced scattering intensity at scattering angle θ. The instrument was calibrated by the usual method, with toluene at 25 °C as the reference liquid. The Rayleigh ratio of pure filtered toluene at 25 °C and 632.8 nm was taken to be 1.406×10^{-5} cm^{-1}. The normalization of the detectors and determination of the interdetector volume were performed with standard monodisperse pullulan ($M_w/M_n = 1.1$) with the molecular weight of 1.18×10^4 g/mol that did not show angular dependence of the light scattering signal. The specific refractive index increments (dn/dc) of Lentinan in water and DMSO were measured by using Optilab refractometer (DAWN® DSP, Wyatt Technology) at 633 nm and 25 °C and found to be 0.140 and 0.060 mL/g, respectively. Astra software (Version 4.70.07) was utilized for data acquisition and analysis.

2.4. Rheological measurements

The dynamic viscoelastic behaviors of Lentinan fractions were carried out on ARES-RFS III rheometer (TA Instruments, USA). A double-concentric cylinder geometry ($R_1/R_2 = 32$ mm/34 mm) was used to measure dynamic parameters such as the shear storage modulus (G') and loss modulus (G'') as functions of angular frequency (ω) at 25 °C. The rheometer was equipped with two force transducers allowing the torque in the range from 0.004 to 1000 g cm. Dynamic strain sweep measurements were carried out at 1 rad/s to determine the linear viscoelastic regime of Lentinan fraction in water with a strain range from 0.1 to 900% for Lentinan fractions in water. Dynamic frequency sweep measurements of G' and G'' were performed in a controlled-strain mode. For each dynamic frequency sweep measurement, a fresh Lentinan fraction solution was prepared and poured into the couette geometry instrument. Temperature control was established by a julabo FS18 cooling/heating bath kept within ±0.4 °C over an extended time. The solution was covered with a thin layer of low-viscosity silicone oil in order to prevent dehydration during rheological measurements.

3. Results and discussion

3.1. Molecular characteristics of Lentinan

Fig. 1 shows the SEC/MALLS chromatogram for Lentinan fraction LF-3 in water. It clearly appears that fractions with highest molecular weight were eluted approximately at the same elution time, leading to the non-Gaussian curve. This is indicative of the dead time, implying that the columns may not be the best condition to work for the sample having high molecular weight and stiff chain conformation. However, their molecular weight was detected by LLS, an absolute method, so it is not a problem for the global weight-average molecular weight determination. This result also suggests that the chains of the sample adopt expanded conformation in water, leading to the large exclusion volume. It is worth noting that the plot of (Kc/R_θ) vs $\sin^2(\theta/2)$ for experimental data becomes practically nonlinear in a broad angular range yielding $\langle s^2\rangle^{1/2}$ unreliably when the molecular weight of sample is greater than 1×10^6 or the sample shows stiffness or the distribution of molecular weight is polydispersed [28,29]. Fig. 2 shows angular dependence of $(Kc/R_\theta)^{1/2}$ for Lentinan fraction LF-3 at a concentration of 1.194×10^{-5} g/mL in water. Obviously, the scattering envelopes in Fig. 2 show a nonlinear angular dependence that has noticeable downward curvature at high angles. Similar curvatures were also found at other concentrations and for other Lentinan fractions in water, which may be attributable to the multiple reasons such as high molecular weight, chain stiffness and polydispersity of molecular weight distribution. Fig. 3 shows the Zimm plot of Lentinan fraction LF-1 in DMSO. The downward curvatures were also observed at high angles. It can be explained as the polydispersity and the extension of polymer chains due to the exclusion volume effect of flexible chains. Table 1 summarizes the intrinsic viscosities [η] and weight-average molecular weight M_w of Lentinan fractions from capillary viscometer and light scattering. Obviously, the values of [η] in water much higher than those in DMSO, and the ratios of [η] in water to that in DMSO are higher than 5, indicating

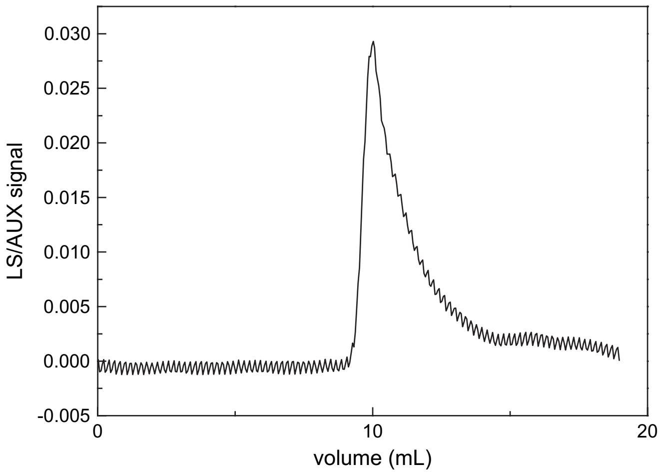

Fig. 1. SEC/MALLS curve of LF-3 in water at 25 °C.

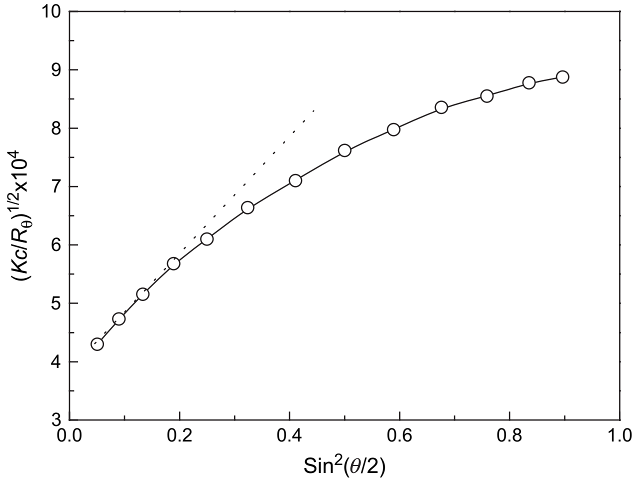

Fig. 2. Angular dependence of $(Kc/R_\theta)^{1/2}$ for LF-3 with a concentration of 1.194×10^{-5} g/mL in water at 25 °C. The dashed line indicates the initial slope.

that Lentinan fraction chains exist in completely different conformation in the two solvents. The higher viscosity in water than in DMSO implies that Lentinan fraction exists as stiff chains in water and flexible chains in DMSO, resulting in a sharp decrease in intrinsic viscosity. The relationships between $[\eta]$ and M_w of Lentinan fractions in water and DMSO are estimated roughly as follows.

$$[\eta] = 2.0 \times 10^{-4} M_w^{1.1} \quad \text{(in water)} \tag{6}$$

$$[\eta] = 9.9 \times 10^{-3} M_w^{0.72} \quad \text{(in DMSO)} \tag{7}$$

The exponents 1.1 and 0.72 further proved that Lentinan fractions show considerable stiffness in water and flexibility in DMSO, in consistency with our previous studies [9,10]. It is well known that the Mark–Houwink exponent α is also related to the reverse of a fractal dimension d_f as follows [30].

$$d_f = 3/(1+\alpha) \tag{8}$$

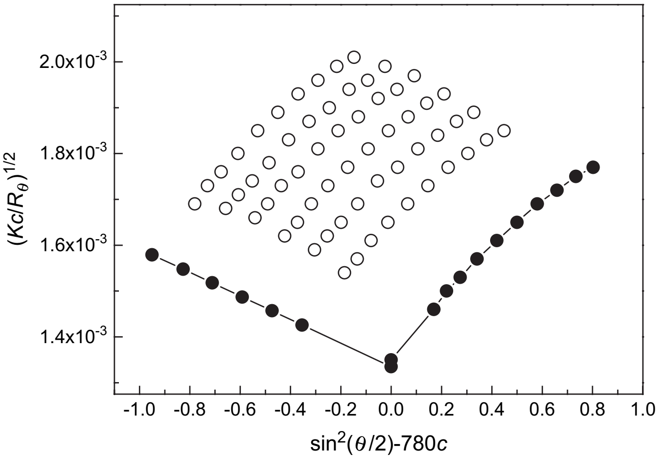

Fig. 3. Zimm plot of LF-1 in DMSO at 25 °C.

Table 1
Molecular characteristics of Lentinan

Samples	$[\eta]$ (mL/g)		$M_w \times 10^{-4}$		$M_{w,\text{ in water}}/M_{w,\text{ in DMSO}}$	$[\eta]_\text{in water}/[\eta]_\text{in DMSO}$
	In water	In DMSO	In water	In DMSO		
LF-1	906.9	128.3	160.1	52.0	3.1	7.1
LF-2	820.8	114.2	141.2	44.4	3.2	7.2
LF-3	744.3	102.9	129.7	38.8	3.3	7.2
LF-4	459.9	80.3	97.5	27.1	3.6	5.7

From Eq. (8), d_f of Lentinan fractions in DMSO can be calculated to be 1.74, revealing that DMSO is a good solvent for Lentinan fractions and the polysaccharides exist as extended coil chains in DMSO [31].

3.2. Dependence of dynamic viscoelastic behavior on concentration

Fig. 4 shows the shear storage moduli (G') and loss moduli (G'') as a function of angular frequency for Lentinan fraction LF-1 with various concentrations c. It is very interesting that Lentinan fraction LF-1 is easily gelled at low concentration (lower than 4.0×10^{-3} g/mL), whereas few general polymers show similar phenomenon. At a concentration of 3.0×10^{-3} g/mL, G' and G'' crossed-over at intermediate frequency, indicative of concentrated solution or viscoelastic fluids or entangled system [32]. This frequency-dependence of G' and G'' can be explained as follows. At relatively low frequencies, where substantial disentanglement of polymer chains can occur easily during the long period of oscillation, the predominant response to the imposed deformation is characterized by the viscous storage G''; at relatively high frequencies, as the rate of oscillation exceeds the timescale of molecular rearrangements, entanglement coupling becomes less distinguishable from "permanent" association of chains in the gel

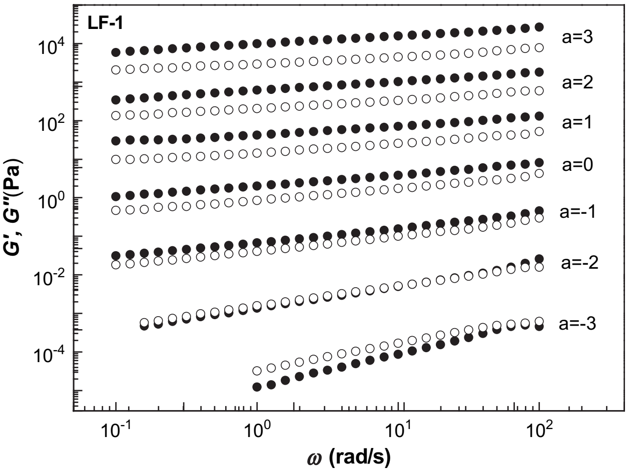

Fig. 4. Storage modulus G' (solid symbols) and loss modulus G'' (open symbols) as a function of angular frequency ω for LF-1 solutions at 25 °C. The concentrations are 2×10^{-3}, 3×10^{-3}, 4×10^{-3}, 5×10^{-3}, 6×10^{-3}, 7×10^{-3} and 8×10^{-3} g/mL from bottom to top. The data were shifted along vertical axes by 10^a to avoid overlapping.

network, and plays a role of knots and forms a temporary three-dimensional network, resulting in the overall response approaching that of a gel where G' predominates [32–35]. Moreover, the crossover frequency decreases with increasing concentration, showing the ability of temporary network is enhanced by an increase in polysaccharide concentration. At a concentration of 4.0×10^{-3} g/mL, the spectra have an obvious weak gel-like character, showing that G' parallels to G'' and dominates over G'' over the entire frequency range examined, but that both moduli still show a frequency-dependence [32]. Based on the above experimental results, it can be concluded that the solution–gel transition occurred between 3.0×10^{-3} and 4.0×10^{-3} g/mL. When c is further increased, the frequency-dependence of G' and G'' becomes weaker and weaker and the value of G' and G'' also increase with increasing concentration, suggesting an increase of the gel strength.

It has been reported that the exponent "n" of $G' \propto \omega^n$, another rheological parameter given by the slope of the log–log plot of G' vs ω, can be used to describe the solution–gel transition. Fig. 4 gives nearly straight lines for log G' vs log ω over the accessible frequency window (three decimal), following the commonly observed relation $G' \propto \omega^n$. The values of exponent n show significant concentration-dependence (as shown in Fig. 5). For n is around 1, the system behaves like a weak gel, while when n tends to 0, the gel presents an elastic behavior [21,36]. In our case, n varies within 0–1, suggesting that Lentinan fraction LF-1 solutions tend to form elastic gels with increasing concentration. The gel strength increases with increasing concentration, as observed from the decrease in the "n" value, in consistency with the result from Fig. 4.

Tan δ is a measure of the relative contribution of viscous components to the mechanical properties of the material. For a conventional elastic gel, $\tan\delta < 0.1$, while for a typical weak gel, the moduli exhibit relatively large frequency-dependence accompanied by a tan δ value >0.1 [37–39]. The G' in Fig. 4 and the corresponding G'' values have been used to estimate the values of tan δ for Lentinan fraction LF-1 at various concentrations. Fig. 6 shows frequency-dependence of tan δ at various concentrations for Lentinan fraction LF-1 in water. Except for the lower two concentrations, the tan δ shows frequency-independence almost in the whole frequency range examined, revealing formation of gels [21,40]. The tan δ values are smaller than 1.0 but slightly higher than 0.1 over the entire frequency range, suggesting that Lentinan fraction LF-1 formed weak gels where the elasticity dominates these systems [41].

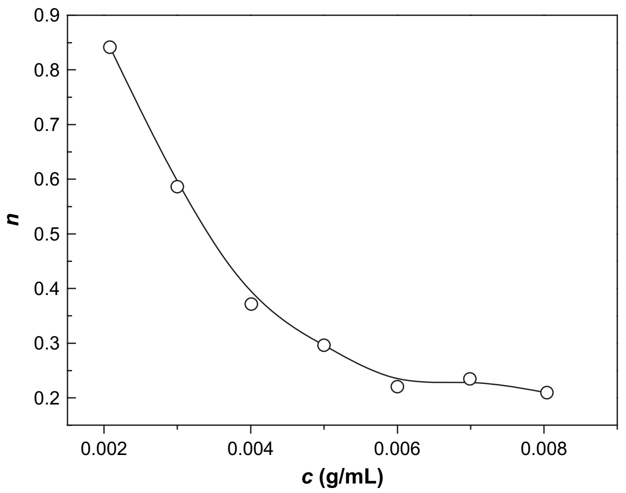

Fig. 5. Exponent n of $G' \sim \omega^n$ as a function of concentration for LF-1 in water at 25 °C.

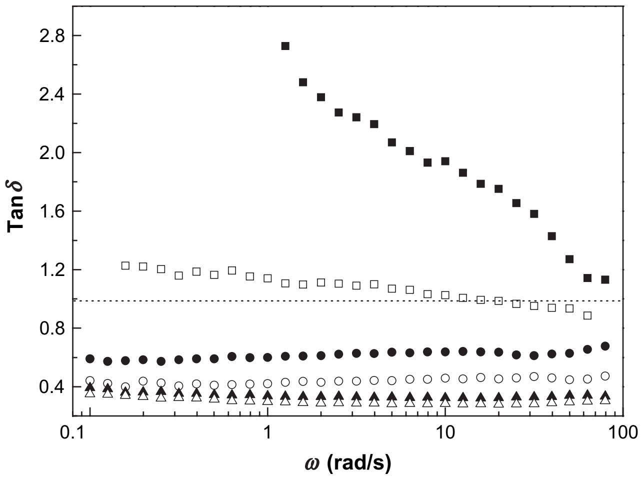

Fig. 6. Loss tangent tan δ as a function of frequency for LF-1 in water at 25 °C and various concentrations. The concentrations are 2×10^{-3}, 3×10^{-3}, 4×10^{-3}, 5×10^{-3}, 6×10^{-3} and 8×10^{-3} g/mL from top to bottom.

The similar dynamic viscoelastic behaviors were observed for the other Lentinan fractions LF-2 and LF-3 as shown in Figs. 7 and 8, and the gelation concentrations where the solution–gel transition occurred were strongly dependent on the molecular weight of Lentinan fractions. Fig. 9 shows G' and G'' as a function of angular frequency for Lentinan fraction LF-4 solutions with various concentrations. In contrast to

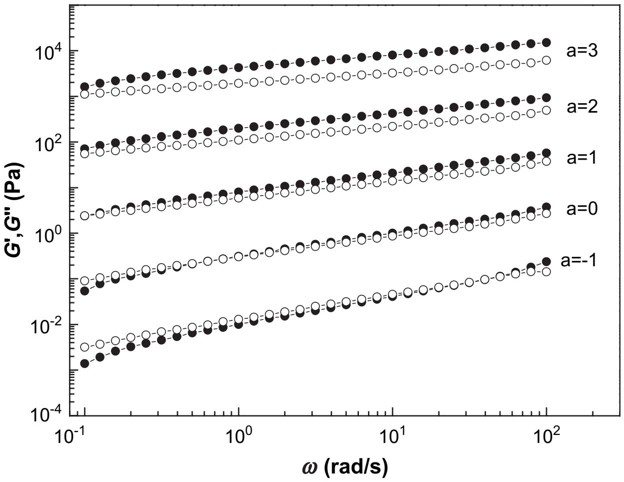

Fig. 7. Storage modulus G' (solid symbols) and loss modulus G'' (open symbols) as a function of angular frequency ω for LF-2 solutions at 25 °C. The concentrations are 3×10^{-3}, 4×10^{-3}, 5×10^{-3}, 6×10^{-3} and 7×10^{-3} g/mL from bottom to top. The data were shifted along vertical axes by 10^a to avoid overlapping.

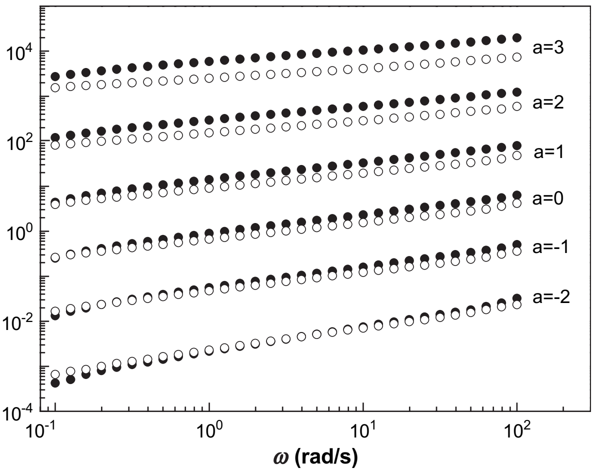

Fig. 8. Storage modulus G' (solid symbols) and loss modulus G'' (open symbols) as a function of angular frequency ω for LF-3 solutions at 25 °C. The concentrations are 4×10^{-3}, 5×10^{-3}, 5.5×10^{-3}, 6×10^{-3}, 7×10^{-3} and 8×10^{-3} g/mL from bottom to top. The data were shifted along vertical axes by 10^a to avoid overlapping.

Lentinan fractions LF-1, LF-2 and LF-3, LF-4 show completely different dynamic rheological behavior. G' and G'' crossed-over at a given frequency indicative of a concentrated solution or an entangled system [32]. At a concentration of 1.0×10^{-2} g/mL, the exponents n of the scaling relation: $G' \sim \omega^n$ and $G'' \sim \omega^n$ at low frequency are 2 and 1, respectively, indicative of a typical liquid-like terminal behavior [42,43]. At a concentration higher than 1.0×10^{-2} g/mL, the frequency-dependence of G' and G'' became weak, and the values of n deviated from 2 and 1, which resulted from the formation of network in water. However, the continuous network or gel formation for Lentinan fraction LF-4 was not observed in the range of concentration used in this experiment. It can be explained as follows: when molecular weight decreased, the chain stiffness increased and the trend of entanglement or aggregation decreased resulting in the weakness of gelation.

Fig. 10 demonstrates the angular frequency of dynamic complex viscosity, η^* of Lentinan fraction LF-1 at different concentrations. Obviously, no marked frequency-independence of η^* was observed for all the polysaccharide systems with different concentration. With increasing concentration, η^* gave a rapid rise and exhibited marked shear-thinning behavior at high angular frequency. Moreover, the critical angular frequency where the shear-thinning behavior occurred, decreased with increasing concentration, which was attributable to the orientation of stiff chain under shear. Doi and Edwards has shown theoretically that rod-like molecules in solution will align and move longitudinally in a constrained tube before the occurrence of intermolecular interaction under the application of shear forces [44], namely, the shear force dominates the Brownian motion, causing molecular alignment, and results in the shear-thinning behavior at low frequency.

3.3. Dependence of dynamic viscoelastic behavior on molecular weight

Fig. 11 shows G' as a function of angular frequency for Lentinan fractions in water with different molecular weight at desired concentration. G' increases with increasing molecular weight at given concentration. The slope of $\log G' \sim \log \omega$ over the entire frequency range decreases sharply with increasing molecular weight. At low frequency, G' of Lentinan fraction LF-1 is distinguishable from those of Lentinan fractions LF-2 and LF-3, and shows very weak frequency-dependence, indicating the formation of Lentinan fraction LF-1 gels and higher strength of the gels.

Fig. 12 shows the frequency-dependence of dynamic complex viscosity η^* of Lentinan fractions in water with different molecular weight. η^* increases abruptly with increasing molecular weight at desired concentration, and frequency-independence was not observed over the entire frequency range for all the LF-series. At a concentration of 4.0×10^{-3} g/mL, η^* of Lentinan fraction LF-1 was much higher than that of

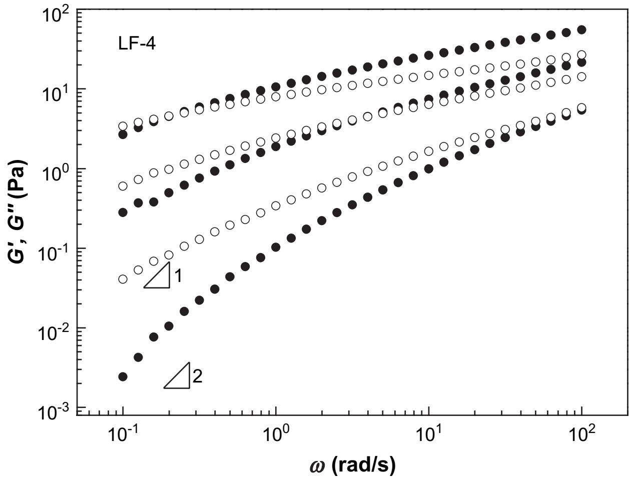

Fig. 9. Storage modulus G' (solid symbols) and loss modulus G'' (open symbols) as a function of angular frequency ω for LF-4 solutions at 25 °C. The concentrations are 1×10^{-2}, 1.5×10^{-2} and 2×10^{-2} g/mL from bottom to top.

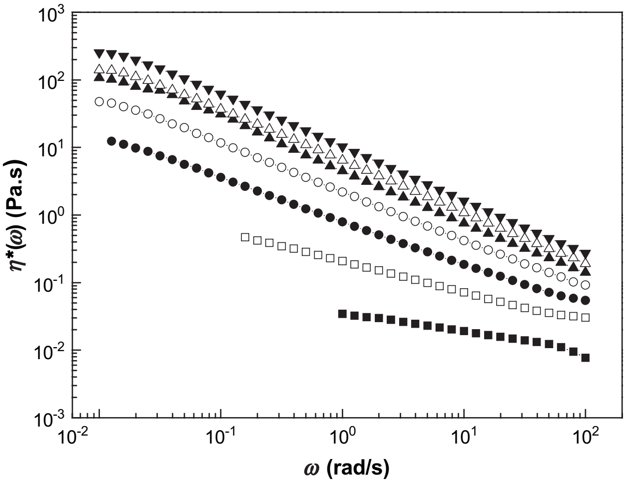

Fig. 10. Complex viscosity η^* as a function of angular frequency for LF-1 in water at 25 °C. The concentrations are 2×10^{-3}, 3×10^{-3}, 4×10^{-3}, 5×10^{-3}, 6×10^{-3}, 7×10^{-3} and 8×10^{-3} g/mL from bottom to top.

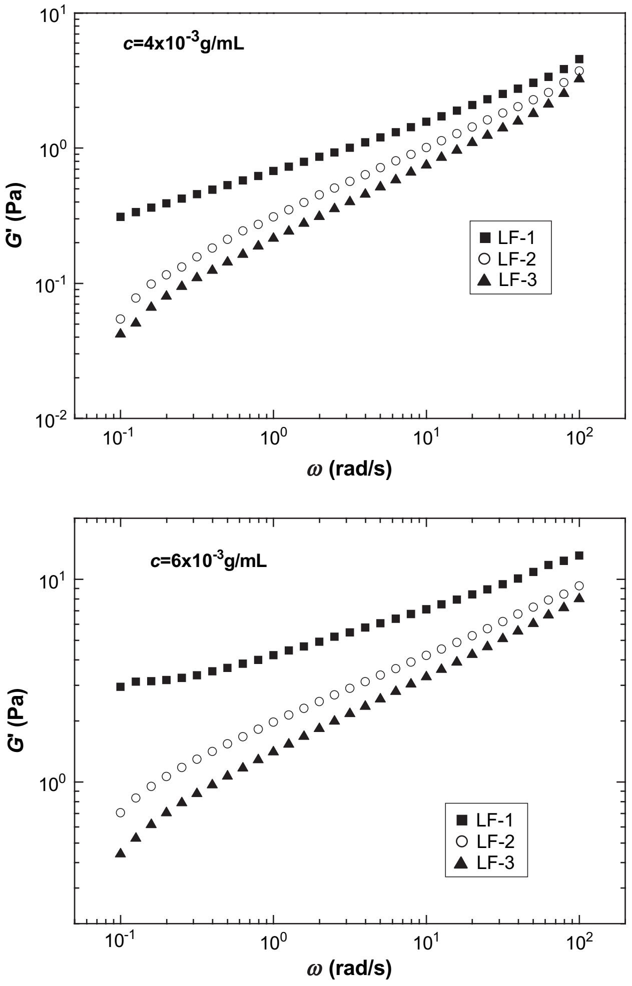

Fig. 11. Storage modulus G' as a function of angular frequency ω for LF-series in water with concentrations of 4×10^{-3} and 6×10^{-3} g/mL at 25 °C.

Lentinan fractions LF-2 and LF-3 at low frequency, but close to each other at high frequency. It can be explained as follows: Lentinan fraction LF-1 with higher molecular weight has formed continuous gel network structure in water because of the concentration larger than its c_{gel} resulting in the much higher viscosity than Lentinan fractions LF-2 and LF-3. At higher concentration of 7.0×10^{-3} g/mL which is higher than the c_{gel} of the Lentinan fractions, the shear-thinning behavior became more strong, and η^* shows no marked difference between the samples having different molecular weights. It can be attributed to the formation of continuous network for all the chains in solution.

3.4. Determination of the critical gelation concentration

As mentioned in Section 1, the scaling law in Eq. (2) at the gel point gives access to determination of the gel point such as the critical gelation concentration [23,45,46] or the critical gelation temperature [47,48]. Furthermore, Eq. (2) enables establishment of the following relation [21]

$$G''(\omega)/G'(\omega) = \tan\delta = \tan(n\pi/2) \qquad (9)$$

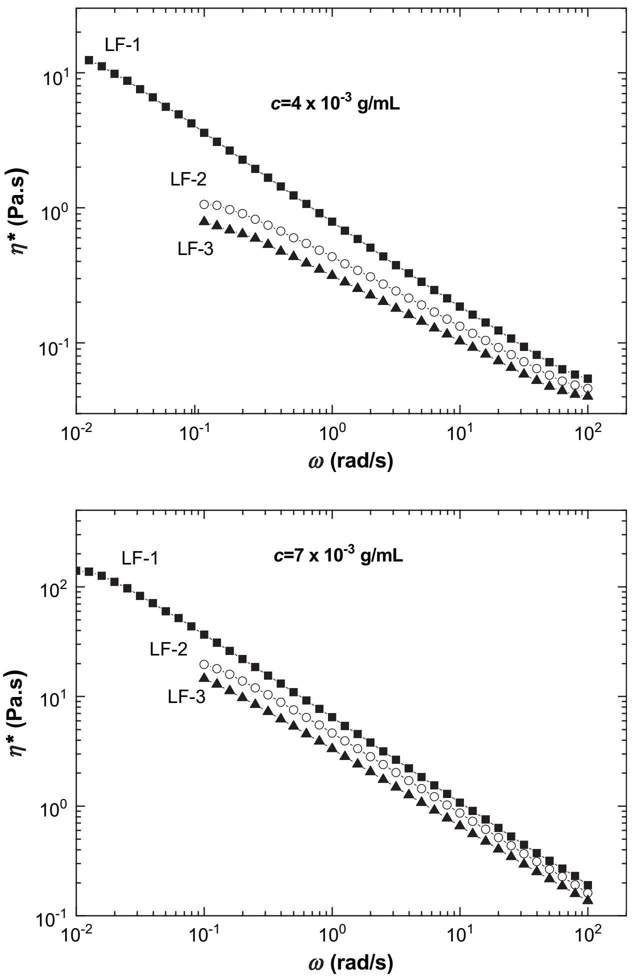

Fig. 12. Dynamic complex viscosity η^* as a function of angular frequency ω for LF-series in water with concentrations of 4×10^{-3} and 7×10^{-3} g/mL at 25 °C.

This frequency-independence of loss tangent in the vicinity of the gel point has been widely used to determine the gel point for chemical and physical gels. In this work, we also examine this method for determining the solution–gel transition

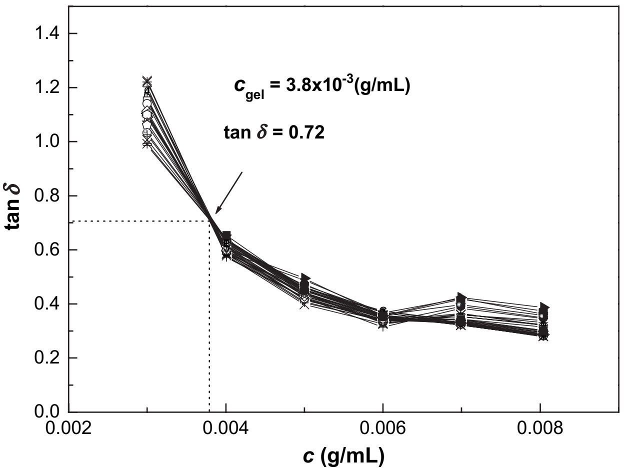

Fig. 13. Loss tangent tan δ as a function of polysaccharide concentration c for LF-1 in water at 25 °C and various angular frequencies. c_{gel} is the gel point.

Table 2
The gel point c_{gel} for Lentinan fractions in water at 25 °C

Samples	$c_{gel} \times 10^3$ (g/mL)
LF-1	3.8
LF-2	6.9
LF-3	7.0

concentration of Lentinan gels from a multifrequency plot of tan δ vs polysaccharide concentration for Lentinan fraction LF-1 in water as illustrated in Fig. 13. All curves have passed through the common point at a certain concentration, which is defined as the gel point or critical gelation concentration c_{gel} and determined to be 3.8×10^{-3} g/mL. As shown in Fig. 6, at a concentration equal to or higher than 4.0×10^{-3} g/mL, tan δ shows frequency-independence suggesting that gel formation occurred. Furthermore, tan δ values are below 1 during the entire gelation process suggesting that the system possesses the weak gel property [49], different from the tan δ values (higher than 1) for chemically cross-linking gel [23]. The value of tan δ at the gel point provides the information about the scaling exponent n of Eq. (2), and then directly obtained $n = 0.4$ by using the relation (9). This value of n is smaller than that (0.75) of poly(vinyl chloride) gels [23], which may be attributed to the higher molecular weight and the presence of extremely entangled triple helix [49]. Additionally, the exponent n is slightly higher than that of Lentinan fraction LF-1 system with concentration of 4.0×10^{-3} g/mL as shown in Fig. 2, implying that the gel point lies in the vicinity of 4.0×10^{-3} g/mL. Additionally, frequency-independence of loss tangent is observed for other Lentinan fractions, and the values of c_{gel} are summarized in Table 2. In order to observe the solution and gel status of Lentinan fraction in water directly, desired amount of Lentinan fraction LF-1 was weighed to prepare the Lentinan/water system with concentration of 6.0×10^{-3} g/mL at 25 °C, which is much higher than the c_{gel} ($\sim 3.8 \times 10^{-3}$ g/mL). The system was stirred continuously until all samples were dissolved completely, and then held still at 25 °C exhibiting clear gel-like state as shown in Fig. 14b. After taking picture of the gel, it was diluted by adding desired amount of water to prepare Lentinan fraction LF-1 solution with concentration of 3.0×10^{-3} g/mL and stirred continuously again. The gel was broken gradually and turned into clear solution as shown in Fig. 14a. This experiment proved that the solution–gel transition behavior of Lentinan fraction LF-1 occurred in water at 25 °C by changing the polymer concentration.

From the above analysis, Lentinan fractions LF-1, LF-2 and LF-3 with relatively high molecular weight form gels at low concentration, showing different solution behaviors from other stiff polysaccharides such as xyloglucan, gellan gum, xanthan gum, schizophyllan and so forth, which will not form gels by itself at any concentration and room temperature but do form when mixed with certain components. Furthermore, the c_{gel} is very low compared to synthesized polymers [23], suggesting that there is stronger intermolecular interaction in Lentinan/water system. As shown in Table 2, the c_{gel} values increase with decreasing molecular weight. Especially when M_w is 84.7×10^4 g/mol, the c_{gel} values increase sharply. For the triple helical Lentinan in water, the increase of molecular weight resulted in the decrease of c_{gel}, namely, the trend of aggregation or entanglements strengthened. This may be attributed to the increases of chain flexibility with increasing molecular weight, resulting in the increase of entanglements and the length of building blocks for gelation.

3.5. Gelation mechanism of Lentinan in water

In order to examine the nature of the structure in Lentinan gels and clarify the gelation mechanism, dynamic strain sweep measurements for Lentinan fraction LF-1 in water with concentration of 6.0×10^{-3} g/mL were repeated for three runs. Moreover, the second and third runs of dynamic strain sweep measurements were done immediately after the end of the former run during which structures in samples had been broken due to large deformation. Fig. 15 shows the results of the above experiments. At the concentration of 6.0×10^{-3} g/mL, the gelation has already happened and the system is in the gel state. From Fig. 15, it can be seen that both G' and G'' keep constant until strain ≈ 100%, beyond which G' and G'' decrease sharply resulting from the structure breaking due to large deformation. Therefore, the strain of 100% can be taken as the upper limit of the linear viscoelastic regime of the

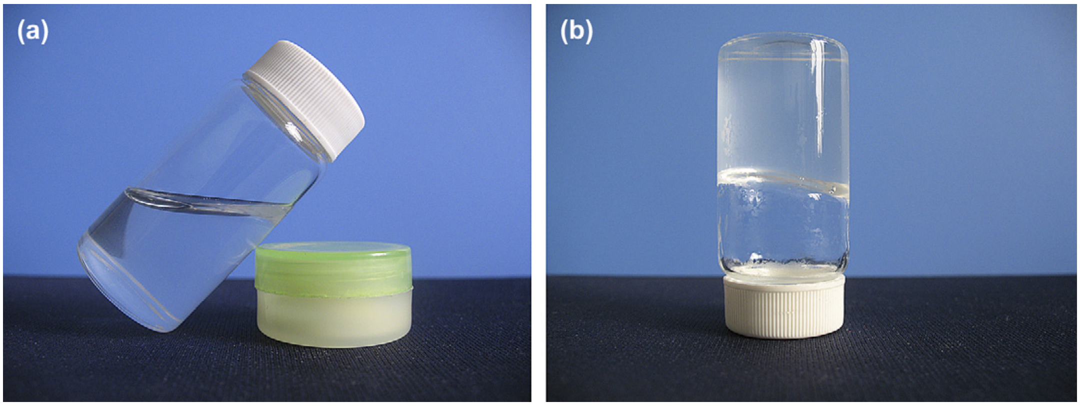

Fig. 14. Photographs of LF-1 with different concentrations of 3.0×10^{-3} g/mL (a) and 6.0×10^{-3} g/mL (b) at 25 °C.

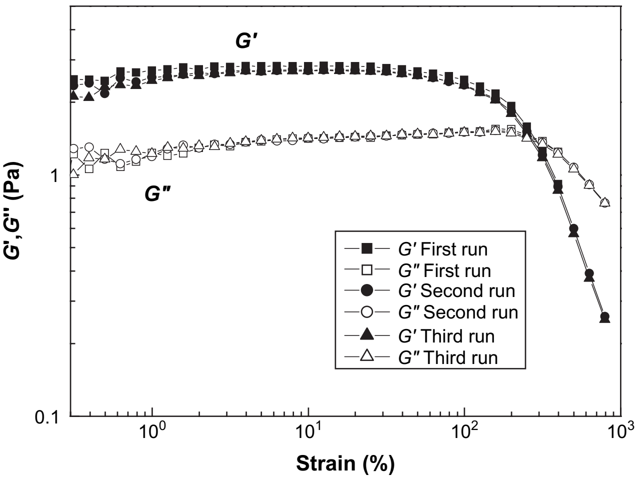

Fig. 15. Strain dependence of G' and G'' determined by dynamic strain sweep measurement at 1 rad/s for Lentinan fraction LF-1 in water at 25 °C. The polysaccharide concentration is 6×10^{-3} g/mL.

present Lentinan gels, which is much higher than that (10%) of (0.8%) schizophyllan–(42%) sorbitol gels [49], revealing that Lentinan has more strong ability to form gels in water than the similar triple helical polysaccharide schizophyllan. As for the results of repeated runs, both G' and G'' determined in the second and third runs are almost the same as those determined in the first run. The good reproducibility of G' and G'' during the repeated experiments reveals that the network structure in Lentinan gels is not permanent and can recover immediately even if the existing structure was disrupted almost completely in the former runs. Additionally, it implies that no junction zones exist in the Lentinan gels; otherwise G' and G'' are irreproducible after large deformation, similar to the gelation behavior of schizophyllan–sorbitol aqueous solution [49].

Moreover, dynamic frequency sweep measurements for Lentinan fraction LF-1 in water with concentration of 6.0×10^{-3} g/mL were also repeated for two runs. The first run was done from low to high frequency, and the second run was performed from high to low frequency immediately after the end of the former run. The results are shown in Fig. 16. Obviously, both G' and G'' in the first run coincide well with those obtained in the second run over the entire frequency range, and no hysteresis was observed. This result suggests that there is no time dependence in the examined frequency range for Lentinan/water gel system.

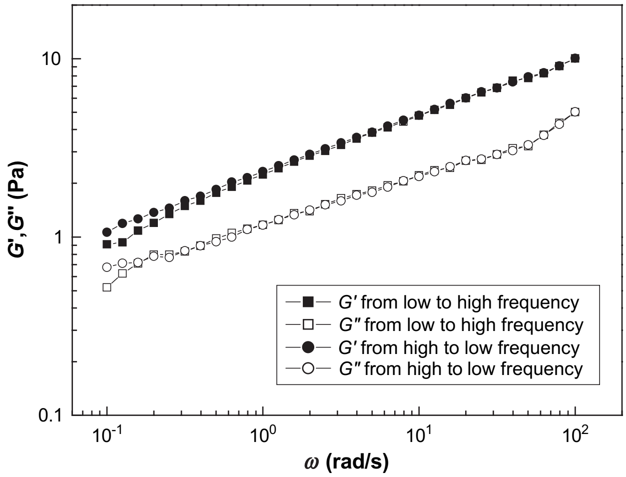

Fig. 16. Frequency-dependence of G' and G'' determined by dynamic frequency sweep measurement at a strain of 1% for Lentinan fraction LF-1 in water at 25 °C. The polysaccharide concentration is 6×10^{-3} g/mL.

4. Conclusion

The solution–gel transition of Lentinan, a triple hehical β-(1 → 3)-D-glucan, in water at 25 °C was observed rheologically. The gel point c_{gel} was determined by using the Winter–Chambon method (frequency-independence of tan δ in the vicinity of the solution–gel transition). It was found that the Winter–Chambon criterion worked well in determining the critical gelation point of the present system although the system behaved as a weak gel before gelation. The c_{gel} was relatively lower than some synthesized polymers and other flexible polysaccharides, resulting from the high stiffness of triple helix and strong aggregation as a result of abundant hydroxyl groups. The c_{gel} decreased sharply with increasing molecular weight. G' and G'' were found to follow a power law behavior as a function of frequency ($G' \sim \omega^n$), and the exponents n are strongly dependent on concentration and molecular weight. The Lentinan solution exhibited shear-thinning behavior at low frequency because of the orientation of the stiff chains under shear force. Compared to the non-gelling Xanthan gum and schizophyllan, Lentinan could form gels more easily at low concentration. The gelation mechanism for Lentinan fraction in water is proposed as follows: the extremely entangled Lentinan chains make a continuous network, conferring to the system the gel-like properties. The structure of Lentinan gel has been proven not to contain junction zones. The Lentinan aqueous gel is more like a very concentrated solution that is unable to flow within a timescale of usual observation. The unique rheology of Lentinan in water would have wide application in industries such as food, pharmaceutical, cosmetics, oil recovery and so on.

Acknowledgements

We gratefully acknowledge the financial support from the National Natural Science Foundation (20404010), the major grant of the National Natural Science Foundation (30350850) of China, and the High-Technology Research and Development Program of China (2006AA02Z102).

References

[1] Dubin P, Bock J, Davies RM, Schulz DN, Thies C. Macromolecular complexes in chemistry and biology. Berlin: Springer; 1994.
[2] Glass JE. Associating polymers in aqueous media. In: ACS Symp Ser 765. Washington, DC: Am Chem Soc; 2001.
[3] Nishirari K, Takahashi R. Curr Opin Colloid Interface Sci 2003;8: 396–400.
[4] Lundin L, Hermansson AM. Carbohydr Polym 1995;26:129–40.

[5] Mannion RO, Melia CD, Launay B, Cuvelier G, Hill SE, Harding SE, et al. Carbohydr Polym 1992;19:91–7.

[6] Tako M, Asato A, Nakamura S. Agric Biol Chem 1984;48:2995–3000.

[7] Zhan DF, Ridout MJ, Brownsey GJ, Morris VJ. Carbohydr Polym 1993;21:53–8.

[8] Zhang P, Zhang L, Cheng S, Zhang P. Biosci Biotech Biochem 1999;63(7):1197–202.

[9] Zhang L, Zhang X, Zhou Q, Zhang P, Zhang M, Li X. Polym J 2001;33:317–21.

[10] Zhang L, Li X, Zhou Q, Zhang X, Chen R. Polym J 2002;34:443–9.

[11] Zhang X, Xu J, Zhang L. Biopolymers 2005;78(4):187–96.

[12] Nishinari K, Zhang H, Ikeda S. Curr Opin Colloid Interface Sci 2000;5:195–201.

[13] Flory PJ. Principles of polymer chemistry. Ithaca, NY: Cornel University Press; 1953.

[14] (a) Stockmayer WH. J Chem Phys 1943;11:45–55;
(b) Stockmayer WH. J Chem Phys 1944;12:125–31.

[15] de Gennes PG. Scaling concepts in polymer physics. Ithaca, NY: Cornel University Press; 1979.

[16] Martin JE, Adolf D, Wilcoxon JP. Phys Rev Lett 1988;61:2620–3.

[17] Martin JE, Adolf D. Annu Rev Phys Chem 1991;42:311–9.

[18] Li L, Uchida H, Aoki Y, Yao ML. Macromolecules 1997;30:7842–8.

[19] Chambon F, Winter HH. Polym Bull (Berlin) 1985;13:499–503.

[20] Winter HH, Chambon F. J Rheol 1986;30:367–82.

[21] Chambon F, Winter HH. J Rheol 1987;31:683–97.

[22] Scanlan JC, Winter HH. Macromolecules 1991;24:47–54.

[23] Li L, Aoki Y. Macromolecules 1997;30:7835–41.

[24] Izuka A, Winter HH, Hashimoto T. Macromolecules 1992;25:2422–8.

[25] Mours M, Winter HH. Macromolecules 1996;29:7221–9.

[26] Li L, Aoki Y. Macromolecules 1998;31:740–5.

[27] Berry GC. J Chem Phys 1966;44:4550–64.

[28] Nakata M. Polymer 1997;38:9–13.

[29] Evans JM. Manipulation of light scattering data. In: Huglin MB, editor. Light scattering from polymer solutions. London and New York: Academic Press; 1972. p. 123 [chapter 5].

[30] Burchard W. Adv Polym Sci 1999;143:113–94.

[31] Gelade E, Goderis B, Koster C, Meijerink N, Benthem R, Fokkens R, et al. Macromolecules 2001;34:3552–8.

[32] Clark AH, Ross-Murphy SB. Adv Polym Sci 1987;83:57–192.

[33] Cui SW. Polysaccharide gums from agricultural products: processing, structure and functionality. Lancaster: Technomic Publishing Company; 2001.

[34] Morris ER. In: Phillips GO, Wedlock DJ, Williams PA, editors. Rheology of hydrocolloids. Gums and stabilizer for the food industry, vol. 2. Oxford and New York: Pergamon Press; 1982. p. 57–77.

[35] Te Nijenhuis K. Viscoelastic properties of thermoreversible gels. In: Burchard W, Ross-Murphy SB, editors. Physical networks: polymers and gels. London: Elsevier Applied Science; 1990. p. 15–33.

[36] Rinaudo M. Food Hydrocolloids 2001;15:433–40.

[37] Ikeda S, Nishinari K. J Agric Food Chem 2001;49:4436–41.

[38] Ross-murphy SB, Morris VJ, Morris ER. Faraday Symp Chem Soc 1983;18:115–29.

[39] Chronakis IS, Piculell L, Borgström J. Carbohydr Polym 1996;31(4):215–25.

[40] Bromberg L. Macromolecules 1998;31:6148–56.

[41] Tuinier R, Oomen CJ, Zoon P, Cohen Stuart MA, de Kruif CG. Biomacromolecules 2000;1:219–23.

[42] Kobayashi K, Huang Ching-I, Lodge TP. Macromolecules 1999;32:7070–7.

[43] Ferry JD. Viscoelastic properties of polymers. 3rd ed. New York: John Wiley & Sons; 1980.

[44] Doi M, Edwards SF. The theory of polymer dynamics. Oxford: Clarendon Press; 1984.

[45] Desbrieres J. Biomacromolecules 2002;3:342–9.

[46] Aoki Y, Li L, Uchida H, Kakiuchi M, Watanabe H. Macromolecules 1998;31:7472–8.

[47] Aoki Y, Li L, Kakiuchi M. Macromolecules 1998;31:8117–23.

[48] Nitta Y, Kim BS, Nishinari K, Shirakawa M, Yamatoya K, Oomoto T, et al. Biomacromolecules 2003;4:1654–60.

[49] Fang YP, Nishinari K. Biopolymers 2004;73:44–60.